Hydrothermal Ion Exchange on Submillimeter-Size Single Crystals of a New Iron(III) Phosphate

Greg Becht and Shiou-Jyh Hwu*

Department of Chemistry, Clemson University, Clemson, South Carolina 29634-0973

Received March 30, 2006
Revised Manuscript Received July 14, 2006

Extended solids that exhibit ion-transport properties are attractive for their potential applications, for example, in fuel cell and battery devices.[1] To investigate chemical transport properties, one would preferentially employ polycrystalline samples to expedite the diffusion process across the interface. While a small-size particle conceivably offers increased surface area in favor of ion transport, it presents fundamental challenges in structure characterization. Often there is a prolonged delay in materials development due to the lack of immediate access to specialized instrumentation, such as solid-state NMR and neutron diffraction, to reveal the ion distribution in resulting solids. To acquire a timely evaluation on chemical transport properties of our newly synthesized materials, we have proceeded with a direct ion exchange on single crystals followed by conventional single-crystal X-ray diffraction (SXRD) methods. The parent compound used in this study was a new iron(III) phosphate $Cs_{4.65(3)}K_{4.35(1)}Fe_7(PO_4)_{10}$, **1**. The direct ion exchange was carried out for the first time, as far as we know, employing mild hydrothermal conditions at 200 °C[2] as opposed to using molten salt at higher temperatures.[3] This approach arose due to the recognition of the interconnected channel structure in **1**. As anticipated, ion exchange does occur readily, and the product exhibits preserved crystal morphology, as shown by the scanning electron microscopy (SEM) photographs in Figure 1. In this report, we will first discuss some background of prior research developments relevant to the study of polyanion-based transition metal oxide materials for battery applications. The communication will then report the results of our exploratory synthesis in the quaternary iron(III) phosphate system and initial studies of ion-exchange reactions of **1**.

Over the past decade, research on positive electrode materials has mainly focused on the layered oxides that are made of close-packed anion lattices. These include $LiCoO_2$ and $LiNiO_2$, the spinel, $LiMn_2O_4$, and variants,[4] which have been commercially adopted as 4.0 V positive-electrode materials for rechargeable lithium batteries. Recently, compounds having complicated three-dimensional frameworks built from XO_4 (X = P, S, V, As, Mo, W)[5,6] polyanions have attracted considerable attention. The studies have revealed that the $M^{n+}/M^{(n-1)+}$ redox couple and in turn the operating voltage of the bulk are tunable by adjusting the polarization of electrons via polyanions. Iron-containing phosphates are among the most studied chemical systems.[7] Compounds subject to structure and property correlation studies include NASICON-type $Li_3Fe_2(PO_4)_3$, pyrophosphates $LiFeP_2O_7$ and $Fe_4(P_2O_7)_3$, and olivine-type $LiFePO_4$.[8,9] Electrochemical analysis has confirmed that the redox couple of Fe^{3+}/Fe^{2+} versus Li/Li^+ occurs at potentials close to 2.8, 2.9, 3.0, and 3.5 V, respectively. Reportedly the inductive effect of the phosphate polyanion diminishes the covalency of the Fe−O bonds, hence increasing the operating voltage of the Fe^{3+}/Fe^{2+} redox couple compared to Fe_2O_3 (1.23 V).[10] It is noted that a distinctly high Fe^{3+}/Fe^{2+} redox potential observed in $LiFePO_4$ was discerned to be a result of fused (edge-shared) FeO_6 octahedra.[7d] The new iron(III) phosphate **1** exhibits channel structures made of polyanion and condensed FeO_n (n = 5, 6) polyhedral units. Hence, we have been prompted to pursue an initial investigation regarding its ion-transport properties.

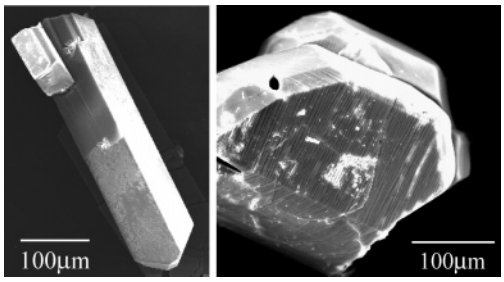

Figure 1. SEM images of single crystals from Rb^+ (left) and Na^+ (right) ion-exchanged reactions. The column and plate-like morphologies of parent crystals were preserved. The Na^+-containing crystal exhibits grooves possibly along certain crystallographic planes; see text.

Employing molten-salt methods, sizable crystals (in amber color) of **1** were grown in column and (thick) plate-like morphologies.[11] **1** crystallizes in the monoclinic space group $P2_1/c$ (No. 14) with the cell dimensions a = 13.898(3) Å, b = 16.381(3) Å, c = 9.835(2) Å, β = 110.45(3)°, and V = 2098(2) Å^3. The X-ray single-crystal structure reveals a three-dimensional framework that consists of interconnected chan-

(1) Whittingham, M. S.; Savinell, R. F.; Zawodzinski, T. *Chem. Rev.* **2004**, *104*, 4243−4244.
(2) Greenblatt, M.; Wang, E. *Chem. Mater.* **1991**, *3*, 542−546.
(3) Edström, K.; Thomas, J. O. *Acta Crystallogr.* **1991**, *B47*, 643−650.
(4) Whittingham, M. S. *Chem. Rev.* **2004**, *104*, 4271−4301 and references cited therein.
(5) Nanjundaswamy, K. S.; Padhi, A. K.; Goodenough, J. B.; Okada, S.; Ohtsuka, H.; Arai, H.; Yamaki, J. *Solid State Ionics* **1996**, *92*, 1−10.
(6) Padhi, A. K.; Nanjundaswamy, K. S.; Masquelier, C.; Goodenough, J. B. *J. Electrochem. Soc.* **1997**, *144*, 2581−2586.
(7) Durif, A. *Crystal Chemistry of Condensed Phosphates*; Plenum Press: New York, 1995.
(8) (a) Salaha, A. A.; Jozwiakb, P.; Garbarczykb, J.; Benkhoujac, K.; Zaghibd, K.; Gendrona, F.; Juliena, C. M. *J. Power Sources* **2005**, *140*, 370−375. (b) Tucker, M. C.; Doeff, M. M.; Richardson, T. J.; Fiñones, R.; Cairns, E. J.; Reimer, J. A. *J. Am. Chem. Soc.* **2002**, *124*, 3832−3833.
(9) (a) Wurm, C.; Morcrette, M.; Rousse, G.; Dupont, L.; Masquelier, C. *Chem. Mater.* **2002**, *14*, 2701−2710. (b) Uebou, Y.; Okada, S.; Egashira, M.; Yamaki, J.-I. *Solid State Ionics* **2002**, *148*, 323−328. (c) Masquelier, C.; Padhi, A. K.; Nanjundaswany, K. S.; Goodenough, J. B. *J. Solid State Chem.* **1998**, *135*, 228−234. (d) Padhi, A. K.; Nanjunclaswamy, K. S.; Masquelier, C.; Okada, S.; Gooclenough, J. B. *J. Electrochem. Soc.* **1997**, *144*, 1609−1613.
(10) (a) Manthiram, A.; Goodenough, J. B. *J. Solid State Chem.* **1987**, *71*, 349−360. (b) Okada, S.; Nanjundaswamy, K. S.; Manthiram, A.; Goodenough, J. B. Presented at the 36th Power Sources Conference, Cherry Hill, NJ, June 6−9, 1994.

10.1021/cm0607482 CCC: $33.50 © 2006 American Chemical Society
Published on Web 08/09/2006

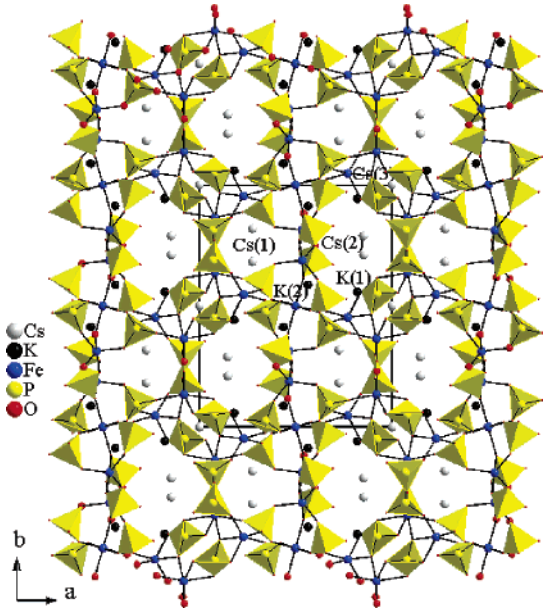

Figure 2. Mixed polyhedral (PO_4) and ball/stick (FeO_n) representations showing the projected view of the $Cs_{4.65(3)}K_{4.35(1)}Fe_7(PO_4)_{10}$ structure along *c*. The cations, K^+ and Cs^+, reside in the channels. The same color codes are applied throughout the report.

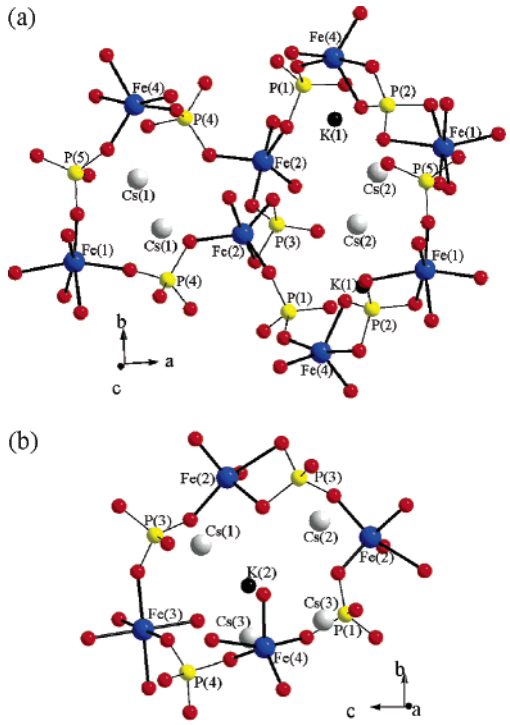

Figure 3. (a) Fused 8- and 12-membered-ring windows for channels viewed approximately along the *c* axis and (b) eight-membered-ring window along the *a* axis. The K^+ and Cs^+ cations residing in the channels are included as a reference for viewing.

nels where the cations K^+ and Cs^+ reside (Figures 2−4). Figure 2 shows the Fe−O−P framework consisting of channels along the *c* axis. One immediately notices the fused windows, which feature 8- and 12-membered rings. The rings consist of edges of vertex- and edge-shared polyhedra, which include three FeO_5 trigonal bipyramids, one FeO_6 octahedron, four PO_4 tetrahedral units, and four FeO_5/two FeO_6/six PO_4 polyhedral units, respectively (Figure 3a). Viewing along the orthogonal axis *a* (Supporting Information, Figure S1), one can recognize an additional set of channels containing an

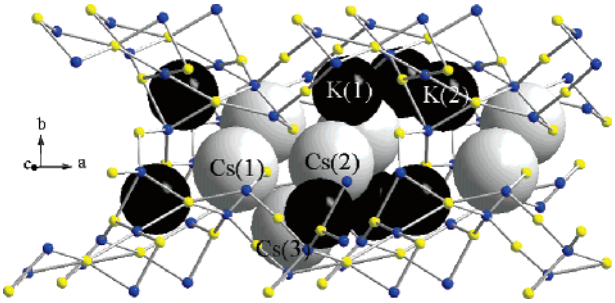

Figure 4. Framework showing the partial structure of interconnected channels along the *a* and *c* directions. The solid lines represent the Fe−P connectivity within the selected distances ranging from 2.66 Å to 3.34 Å. For simplicity, the oxygen atoms are omitted.

eight-membered Fe−O−P window made of three FeO_5/one FeO_6/four PO_4 (Figure 3b).

The channels along the *a* and *c* directions are interconnected as might be discerned from Figure 4. One can see a window in the middle of the drawing facing approximately along the *c* axis and two additional openings at opposite ends along *a*. Judging from the "compaction" of cations, it would be possible for cations to hop between sites, a necessity for the facile ion transport.

It should be pointed out that the nonstoichiometry with respect to the cations K^+ and Cs^+ in **1** is due to the cation disordering on the Cs(2) and Cs(3) sites.[12] On the basis of this preliminary SXRD result, we speculate the existence of a possible solid solution series (Supporting Information, Figure S2). In the meantime, the interconnected channel structure of **1** has attracted us to survey its chemical-transport properties.

Ion-exchange reactions under mild hydrothermal conditions were successful as opposed to using molten nitrate salt. Single crystals (ca. 30 mg) of **1** were immersed in 10 mL of 1 M ANO_3 solutions (A = Li, Na, K, Rb, Cs) and heated in a Teflon-lined hydrothermal bomb at 200 °C for 12 h. Although the morphologies of the crystals were mostly preserved, the plate-like crystals suffered microscopic damage as shown by the apparent grooves seen on the surface of crystals (Figure 1, right). Subsequently, its structural solution (Supporting Information, Table S1) was relatively poor. We believe that a fairly large volume reduction (ca. 0.36% for the Na phase) could also be one of the causes of destruction in crystallinity. We are currently investigating a correlation between the groove formation and crystal-

(11) Single crystals of **1** were synthesized from the mixture (charge) of P_4O_{10} (Aesar, 99.9%), Fe_2O_3 (Aesar, 99.9%), and KO_2 (Aesar, 96.5%) with a molar ratio of 5:3.5:4. An eutectic salt (flux, mp = 621 °C) of 48 mol % KCl (Aesar, 99.995%) and 52 mol % CsCl (Aesar, 99.995%) was ground together in an inert atmosphere dry box. The charge to flux ratio was 1:5 by weight. The mixture was loaded into a carbon-coated silica ampoule and then sealed under vacuum. The reaction was heated to 750 °C at a rate of 2 °C/min, isothermed for 2 days, and finally cooled by 3 °C/min to room temperature. Crystals of **1** (~80% yield) along with $CsK_2Fe_4(PO_4)_5$ were isolated by washing the reaction products with deionized water using a suction filtration method.

(12) The *R* values were improved from 0.077 to 0.052 with Cs(2) and Cs(3) being refined as mixed K/Cs sites as opposed to 95% occupied Cs, assuming there is no redox chemistry taking place during the course of ion exchange. The ultimate solution was confirmed based on the monitored values of the bond valence sum for Fe^{3+} (Supporting Information, Table S4).

lographic planes with respect to possible conduction pathways through which ion transport could take place.

As expected, the substituted alkali metal cations A^+ are statistically distributed over both K^+ and Cs^+ sites in **1**. For each data crystal, the contents were confirmed via semiquantitative elemental analysis by the energy dispersive X-ray (EDX) method using a Hitachi S-3500 scanning electron microscope equipped with an OXFORD EDX microprobe. The refined compositions, according to the employed ANO_3 solution, are $Cs_{5.95(2)}Li_{3.05(1)}Fe_7(PO_4)_{10}$, **2**; $Cs_{4.86(2)}Na_{4.14(1)}Fe_7(PO_4)_{10}$, **3**; $Cs_{5.63(2)}K_{3.37(1)}Fe_7(PO_4)_{10}$, **4**; $Cs_{4.25(3)}Rb_{1.89(1)}K_{2.86(2)}Fe_7(PO_4)_{10}$, **5**; and $Cs_{5.67(1)}K_{3.33(1)}Fe_7(PO_4)_{10}$, **6**; respectively. A close examination of the refinement results of site occupancy shown in Supporting Information, Table S2, suggests that there is a preferred ion substitution. One can distinctly divide the results into two categories according to the relative size of the A^+ cation, that is, smaller ($A^+ = Li^+$, Na^+) versus larger ($A^+ = K^+$, Rb^+, Cs^+). For the K(1) and Cs(1) sites, there is no sign of substitution with larger ions. This is consistent with the tight coordination spheres that these two cations adopt judging from relatively short A−O distances (Supporting Information, Table S2). Other cation sites in **1** are evidently accessible by ions of all sizes via solution.

Seemingly Li^+ substitution on the K(1) and Cs(1) sites occurs less readily than Na^+. This could be because the steric hindrance due to the solvation sphere of $[Li(H_2O)_n]^+$ is larger than that of $[Na(H_2O)_m]^+$, where $n > m$.[13] The K(1) site was then refined as mixed Cs^+/Li^+ in **2**[14] but a fully occupied Na^+ site in **3**.

The ion hopping inside the channel frameworks is thus evident in all ion-exchanged products, and the resulting crystals, with an exception of **5**, possess cesium compositions exceeding the original value of **1**. In **4**, for instance, the structural solution suggests mixed K^+/Cs^+ on the K(2) site, which is presumably due to internal ion transport (diffusion). It is interesting to note that **6** (obtained from the $CsNO_3$ solution) adopts a similar overall composition as **4**. We, however, are uncertain about the source of extra Cs^+ cation in others unless some of the secondary crystals (Supporting Information, Figure S2) were dissolved to provide the needed cesium cations through solution. In **5**, although $[Cs^+]$ was decreased, the overall concentration of large cations (Rb^+ and Cs^+) was increased. In retrospect, the Rb^+ diffusion could also be attributed to the interconnected "open-channel" (Figure 3) where the K^+/Cs^+ cations reside in rather loose coordination environments (Supporting Information, Figure S3) judging from calculated low bond valence sum values (Supporting Information, Table S4).

In final remarks, molten-salt methods have enabled the growth of sizable single crystals for direct ion-exchange studies; the study suggests that this new iron(III) phosphate phase possesses exceptional ion-transport properties worthy of further investigations. **1** reveals an almost perfectly ordered channel structure, which ensures low free energy for ion transport. It should be noted, however, that a good ion-exchange property is a necessary but not sufficient condition for good ionic conductivity.[15] The nonstoichiometry could be due to the result of ions being trapped in the structure under non-equilibirum conditions. We plan to carry out systematic investigations on controlled (time-dependent, for instance) ion exchange and study its correlation with the ionic conductivity as well as electrochemical potential. Employing mixed alkali-metal cations, we anticipate that more fascinating quaternary iron(II,III) phosphates are yet to come. Also, the three-dimensional structure of **1** contains interesting Fe_2O_{10} dimers and Fe_3O_{14} trimers interconnected by PO_4 tetrahedral units (Supporting Information, Figure S4). These fused FeO_n polyhedra have warranted the initial magnetic studies, which will be the subject of another article.[16]

Acknowledgment. The authors gratefully acknowledge continued financial support from the National Science Foundation (NSF) for this research (DMR-0077321, 0322905) and the purchase of the single-crystal X-ray diffractometer (ESR-9108772, CHE-9207230, 9808165).

Supporting Information Available: Tables of selected crystallographic data, A−O bond distances and A-site occupancies, calculated bond valence sums, figures of projected view of **1** along *a*, PXRD patterns, KO_n and CsO_m coordination and connectivity, and partial structure of PO_4-linked Fe_2O_{10} dimers and the Fe_3O_{14} trimer (PDF); an X-ray crystallographic file, in CIF format. This material is available free of charge via the Internet at http://pubs.acs.org.

CM0607482

(13) Cotton, F. A.; Wilkinson, G.; Gaus, P. L. *Basic Inorganic Chemistry*, 3rd ed.; John Wiley & Sons, Inc.: New York, 1995; p 291.

(14) The EDX results show no trace amount of K. Both K^+ sites were by default refined as mixed Cs^+/Li^+ cations to keep the charge balanced according to the calculated oxidation state of Fe^{3+} (Supporting Information, Table S3).

(15) England, W. A.; Goodenough, J. B.; Wiseman, P. J. *J. Solid State Chem.* **1983**, *49*, 289−299.

(16) Becht, G.; Britt, R; Eagle, C. T.; Hwu, S.-J. *Inorg. Chem.*, manuscript in preparation.